

## THERMODYNAMIC CHARACTERISTICS ANALYSIS OF SOLAR HOT WATER HEATING COMPOSITE SYSTEM FOR LOW CARBON HEATING

by

**Zhiying ZHANG, Yanfang MA<sup>\*</sup>, and Jianwei ZHAO**

Shijiazhuang Institute of Railway Technology, Shijiazhuang, Hebei, China

Original scientific paper  
<https://doi.org/10.2298/TSCI2402491Z>

*The low carbon renewable energy complementary cogeneration system has broad application prospects in the field of regional comprehensive energy utilization. The author proposes a trough solar assisted biomass cogeneration system that utilizes medium to low temperature trough solar energy to heat conduction oil and drive an absorption heat pump to preheat the water in the heating network, saving heating and steam extraction and increasing power output while maintaining a constant biomass fuel and heating volume. The EBSILON Professional software was used to model and simulate the case unit and integrated system, and based on this, thermodynamic characteristics such as system energy flow and energy loss were analyzed. The results show that under design conditions, a solar power generation capacity of 1.79 MWh can be generated, with a photoelectric efficiency of 20.07% and a photoelectric conversion efficiency of 21.61%. This can provide theoretical guidance for the research and practical application of solar energy and biomass energy in integrated cogeneration systems.*

**Key words:** *trough solar energy, biomass cogeneration, absorption heat pump, system integration, thermodynamic analysis*

### Introduction

The research on solar hot water heating started relatively early abroad. In the 1940's, the Massachusetts Institute of Technology in the USA began research on heating and air conditioning systems using solar collectors as heat sources, and held academic seminars on the use of solar heating, publishing many academic papers on solar heating [1]. The role of solar heating in promoting development was the invention of flat panel collectors in 1945 and the invention of all glass vacuum tube collectors in 1975. Afterwards, the use of heat collection technology for building heating began to move from the experimental stage to the application stage. In the 1970's, demonstration buildings for active solar houses were built, including the Thomson Sun House in the suburbs of Washington and the Love Sun House in Denver, Colorado [2]. The successful operation of these solar houses indicates that solar heating and air conditioning systems are completely feasible in technology, but due to the large investment, the promotion and popularization of these systems are not as widespread as passive solar houses. In the 1990's, the application range of solar hot water heating systems was expanded due to the development of more efficient solar collectors, absorption chillers, and heat pump units. Compared with foreign countries, the research on solar hot water heating

<sup>\*</sup> Corresponding author, e-mail: 21172347@qq.com

started relatively late in the country, starting after 2000. Between 2010 and 2015, this technology developed from a demonstration project stage to large-scale application. At present, the solar heating technology system is relatively complete, and relevant national standards and technical manuals have also been released and implemented. The research on solar hot water heating mainly focuses on the mathematical model, computer simulation, configuration optimization, and operational parameter optimization of the system. Many domestic and foreign teams are committed to the integration research of renewable energy systems, and it is generally believed that PV and centralized solar energy are one of the most promising RES for development and utilization [3]. At present, four centralized solar power generation technologies have become mature, among which the parabolic trough type has been widely used. In order to improve the low efficiency and high cost of solar thermal power generation, solar assisted power generation technology has attracted the attention of relevant scholars. By using solar energy to heat the thermal fluid instead of partial extraction heat the feedwater, the saved extraction steam continues to expand and do work in the turbine, resulting in additional power generation that can be considered solar power generation. Biomass accounts for approximately 50% of the Earth's renewable energy and is considered another highly promising RES. Therefore, it is necessary to explore the feasibility of applying solar assisted power generation technology to biomass units. Based on the aforementioned background, the author proposes a trough solar assisted biomass cogeneration system that collects heat from solar radiation and is used to drive an absorption heat pump to preheat water in the heating network, saving heating and steam extraction obtain more electricity generation. The fundamental reason for improving system performance has been revealed through energy analysis and thermal analysis. This can provide theoretical guidance for the research and practical application of solar energy and biomass energy in integrated cogeneration systems.

## Methods

### *Case unit introduction*

The author selected a typical biomass cogeneration unit in Region A as a reference case. The high temperature and high pressure steam generated by biomass boilers is subjected to steam turbine power, condensed in the condenser, and then sequentially enters the three-stage low pressure heater, deaerator, and two-stage high pressure heater [4]. During the local heating period (from November 1<sup>st</sup> to March 31<sup>st</sup> of the following year, a total of 151 days), some 3<sup>#</sup> steam is extracted to heat the heating network water in the heating network heater, which is used to provide heat to local residents. During the heating period, 5.57 kg per second of 3<sup>#</sup> steam extraction is used for regional heating, heat the 74.92 kg per second heat supply network return water from 50.0-99.01 °C, providing 15.4 MWh of heat to heat users. The net power generation generated at the same time is 29.99 MWh, and the biomass consumption is 11.83 kg per second. The main raw materials for biomass boilers are corn straw, corn cob, rice straw, and rice husk, with an average low calorific value of 9.436 MJ/kg for fuel.

### *System modelling and simulation*

The author used EBSILON Professional software to model and simulate the case unit and integrated system, which is a software used for thermodynamic modelling in the power generation field [5]. It maintains balance among components, subsystems, and the entire system while ensuring mass and energy conservation. In this software, a thermodynamic cycle is constructed from a non-linear system of equations, solved iteratively through a series of linear equations, and variable coefficients are formed using the previous iteration values. The iteration

stops when the basic variable no longer changes. After verification, this software is a reliable thermodynamic modelling software. Based on the boundary conditions of the case unit, a model was established using the built-in module of EBSILON Professional, and the calculation results were compared and analyzed with the design data of the case unit. The results showed that the simulation model was accurate and reliable.

In order to improve the utilization rate of solar energy and utilize more renewable energy for power generation and heating, the author proposes a trough solar assisted biomass cogeneration system, as shown in fig. 1.

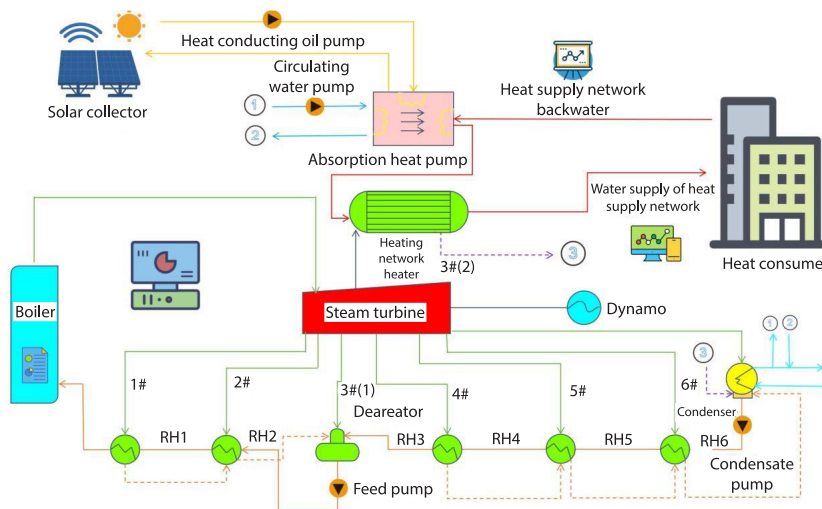


**Figure 1. Schematic diagram of solar assisted biomass cogeneration system**

Firstly, the heat transfer oil that leaves the solar collector serves as the driving heat source and releases heat in the generator of the absorption heat pump. The circulating working fluid absorbs heat and evaporates, and the generated steam condenses in the condenser of the heat pump. After throttling, it flows into the evaporator. Secondly, the low level heat source in the evaporator uses partially exchanged circulating cooling water, and the steam absorbs heat from the circulating cooling water and evaporates. Finally, the saturated steam at low temperature and pressure is sent to the absorber for absorption by the lithium bromide solution [6]. Therefore, the heat discharged by the absorption heat pump in the absorber and condenser can be used to preheat the heating network water supply. Due to the fact that the heating network water obtains energy from the absorption heat pump before the heating network heater, the amount of heat required from the heating network heater decreases, resulting in a decrease in the amount of steam extracted from the 3<sup>#</sup> steam entering the heating network heater. The saved steam extraction can continue to expand and do work in the turbine, while maintaining the same heat supply while increasing the total power generation of the system, achieving the organic integration of solar and biomass renewable energy, thereby making solar energy more effectively utilized.

The solar thermal system adopts the Eurotrough ET-150 commercial parabolic trough collector, which uses 12 collector components. The circulating working fluid uses Thermol VP-1 thermal oil, which is boosted by a thermal oil pump and sent to an absorption heat pump.

## Evaluation indicators

### *Energy evaluation indicators based on the First law of thermodynamics*

Total energy conversion efficiency,  $\eta$ , it is often used to evaluate the overall performance of integrated systems, defined as the ratio of total energy output to total energy input, which characterizes the degree of energy conversion in the integrated system. It can be calculated:

$$\eta_t = \frac{P_{e,t} + Q_{h,t}}{Q_b + Q_s} \quad (1)$$

where  $P_{e,t}$  is the net total power generation,  $Q_{h,t}$  – the net total heating capacity,  $Q_b$  – the input energy of biomass fuel, and  $Q_s$  – the input energy of solar energy. The input energy  $Q_b$  of biomass fuel and the input energy  $Q_s$  of solar energy are calculated:

$$Q_b = Q_{LHV} \times m_b \quad (2)$$

$$Q_s = \frac{I \times A_{SF}}{1000} \quad (3)$$

where  $Q_{LHV}$  is the low calorific value of biomass fuel,  $m_b$  – the amount of biomass fuel,  $I$  – the intensity of direct normal radiation (DNI) from the Sun, and  $A_{SF}$  – the effective optical area of the mirror field. Due to the constant heating capacity of the integrated system and the case unit, the additional electricity generated by the system after the introduction of solar energy can be considered as solar power generation. For integrated systems, solar power generation can be expressed:

$$P_{e,s} = P_{e,t} - P_{e,b} \quad (4)$$

where  $P_{e,b}$  is the biomass power generation, which remains unchanged before and after integration. The PV efficiency  $\eta_{en,s}$  is used to evaluate the utilization rate of collected solar energy:

$$\eta_{en,s} = \frac{P_{e,s}}{Q_s} \quad (5)$$

The average photoelectric efficiency  $\eta_{en,sa}$  during the heating season is used to measure the utilization rate of solar energy collected throughout the entire heating season, which can be calculated:

$$\eta_{en,sa} = \frac{\sum_{k=1}^{3624} P_{s,k}}{\sum_{k=1}^{3624} Q_{s,k}} \quad (6)$$

where  $P_{s,k}$  is the net solar power generation in the  $k$ th hour of the heating season and  $Q_{s,k}$  – the solar input energy in the  $k$ th hour of the heating season [7].

### *Evaluation indicators based on the second law of thermodynamics*

The maximum available energy theoretically obtainable from a system in a given environment can clearly elucidate the location, nature, and cause of energy loss during the process. The total conversion efficiency  $\eta_{ex,t}$  is often used to measure the degree of utilization of system energy:

$$\eta_{ex,t} = \frac{E_e + E_h}{E_b + E_s} \quad (7)$$

where  $E_e$  is the net power generation output,  $E_h$  – the net heating output,  $E_s$  – the input of biomass fuel, and  $D$  – the solar input power.

## Results and discussion

### Integrated system parameters

The integrated system was simulated using EBSILON Professional software, and the basic parameters of the solar thermal system in the design scheme are shown in tab. 1. Choose 15:00 p. m. on March 21<sup>st</sup> as the design point for the integrated system, at which time the DNI is 908.68 W/m<sup>2</sup> and the mirror field efficiency is 52.19%. The heat transfer oil absorbs heat from 123.01-153.01 °C in the collector and is used to drive the absorption heat pump. The circulating cooling water entering the absorption heat pump is cooled from 27.51-25.51 °C. The heat supply network obtains a total of 8.24 MWh of heat from heat transfer oil and circulating cooling water, and the temperature increases from 50.01-76.31 °C. The COP of the absorption heat pump reaches 1.786. The basic parameters of the absorption heat pump are shown in tab. 2 [8].

**Table 1. Basic parameters of solar thermal system**

Parameter	Numerical value
DNI [Wm <sup>-2</sup> ]	908.68
Heat transfer oil inlet (outlet) temperature [°C]	123.01 (153.01)
Heat transfer oil flow rate [kgs <sup>-1</sup> ]	82.38
Solar input [MWh]	8.89
Mirror field efficiency [%]	52.19
Effective energy [MWh]	4.65

**Table 2. Basic parameters of absorption heat pump**

Parameter	Numerical value
Heat transfer oil inlet (outlet) temperature [°C]	153.01 (123.01)
Heat transfer oil flow rate [kgs <sup>-1</sup> ]	82.38
Cooling water inlet (outlet) temperature [°C]	27.51 (25.51)
Cooling water flow rate [kgs <sup>-1</sup> ]	416.68
Heat supply network water inlet (outlet) temperature [°C]	50.01 (76.31)
Heating network water flow rate [kgs <sup>-1</sup> ]	75.92
Heating capacity [MWh]	8.24
COP	1.786

Due to the use of solar thermal systems to assist in heating during the heating season, the parameters of the heating network heater in the integrated system have changed compared to before. Table 3 lists the comparison of the parameters of the heating network heater in the case unit and the integrated system.

In the integrated system, the heating network water supply is preheated in the absorption heat pump before entering the heating network heater, and the water temperature rises from 50.01-76.31 °C. Therefore, the steam extraction volume of 3<sup>#</sup> entering the heating network heater significantly decreased from 5.57-269.01 kg per second, and the thermal load of the heating network heater decreased by 8.23 MWh, a decrease of 53.5% compared to before.

**Table 3. Comparison of parameters of heating network heaters in case units and integrated systems**

Parameter	Case unit	Integrated system	Difference
Inlet temperature of heating network water supply [°C]	50.01	76.31	26.3
Outlet temperature of heating network water supply [°C]	99.01	99.01	0
Heating network water supply flow rate [kgs <sup>-1</sup> ]	74.92	74.92	0
Heating extraction pressure [MPa]	1.14	1.14	0
Heating extraction temperature [°C]	288.11	288.11	0
Heating extraction flow rate [kgs <sup>-1</sup> ]	5.57	2.7	-2.87
Heating and drainage temperature [°C]	60.01	86.31	26.3
Heating and drainage flow rate [kgs <sup>-1</sup> ]	5.57	2.7	-2.87
Heating load of heating network heater [MWh]	15.4	7.17	-8.23

### Energy analysis

The comparison of energy parameters between the case unit and the integrated system is shown in tab. 4 [9]. It can be seen that compared with the case unit, the integrated system has significantly improved the performance of the unit while maintaining a consistent amount of biomass fuel. The heating capacity of the integrated system is still 15.4 MWh, while the net power generation increased by 5.94%. Due to the introduction of solar energy, the total energy conversion efficiency has decreased by 1.52%, and the photoelectric efficiency can reach 20.06%.

**Table 4. Comparison of energy parameters between case units and integrated systems**

Parameter	Case unit	Integrated system	Difference
Biomass fuel quantity [kg/s]	11.83	11.83	0
DNI [W/m <sup>2</sup> ]	–	908.68	–
Solar input [MWh]	–	8.89	–
Total input energy [MWh]	111.55	120.43	8.88
Heating capacity [MWh]	15.4	15.4	0
Net generation [MWh]	29.99	31.77	1.78
Net solar power generation [MWh]	–	1.79	–
Total energy conversion efficiency [%]	40.68	39.16	-1.52
Optoelectronic efficiency [%]	–	20.07	–

Due to the fixed energy input of biomass, it is set as a benchmark value of 100%. In addition, the flow and temperature of the return water and supply water of the heating network remain unchanged before and after integration, so the heating capacity remains constant. Compared to the design of the case unit only heating the heating network water in the heating network heater through 3<sup>rd</sup> steam extraction, in the integrated system, the heating network water is achieved through two steps: absorption heat pump and heating network heater. The heat

transfer oil obtains 4.63 MWh of energy from solar radiation and uses this energy to drive an absorption heat pump. The circulating cooling water serves as a low level heat source, releasing 3.60 MWh of energy in the absorption heat pump. Therefore, if the heating network water supply absorbs 8.23 MWh of heat in the absorption heat pump, the energy absorbed in the heating network heater will be reduced by 8.23 MWh, resulting in a decrease of 2.87 kg per second the required 3<sup>#</sup> steam extraction amount. Therefore, under the condition of maintaining the same heating capacity, the total power generation increased by 2.02 MWh and the net power generation increased by 1.78 MWh.

*Energy analysis*

In order to further explore the root causes of the improvement in unit performance caused by the integration solution, a comprehensive analysis was conducted on the case unit and integrated system, and the results are listed in tab. 5 [10]. Before and after integration, the input of biomass fuel remains constant (considered as 100%), and the losses of biomass boilers remain unchanged. The 8.26 MWh of solar energy is input into the integrated system, and the exhaust steam volume increases with the decrease of heating extraction volume. The thermal losses of steam turbines, condensers, and generators all increase. In addition, due to the heat resource of solar heating system, the heat loss of heating grid system was reduced by 1.77 MW/h, while the heat loss of solar heating system was reduced by 7.35 MW/h. Overall, the power loss of the entire system has increased by 6.49 MWh. Meanwhile, the total output has increased by 1.79 MWh. Although the overall efficiency has decreased by 0.22%, the photoelectric conversion efficiency can reach 21.61%.

**Table 5. Parameters of case unit and integrated system**

Parameter	Case unit		Integrated system	
	Value [MWh]	Ratio [%]	Numerical value [MWh]	Proportion 1%
Biomass input	128.11	100.00	128.11	100.00
Solar input	–	–	8.26	6.45
Total input	128.11	100.00	136.36	106.45
Power generation output	29.99	23.41	31.77	24.791
Heating output commission	2.18	1.691	2.18	1.691
Total output	32.16	25.11	33.94	26.491
Boiler damage	79.35	61.95	79.35	61.95
Steam turbine damage	7.691	6.01	8.25	6.45
Generator damage	0.35	0.28	0.37	0.29
Loss of condenser	1.55	1.21	1.68	1.32
Loss of heat exchanger	0.37	0.29	0.35	0.27
Mirror field damage	–	–	6.98	5.45
Loss of absorption heat pump	–	–	0.38	0.291
Loss of heating network heater	2.98	2.33	1.22	0.95
Auxiliary power	3.71	2.891	3.93	3.07
Total conversion efficiency [%]	25.11		24.89	
Photoelectric conversion efficiency [%]	–		21.61	

## Conclusion

The author selected a typical biomass cogeneration unit in Region A as a reference case. Using EBSILON Professional software for modelling and simulation of case units and integrated systems, this is a software used for thermodynamic modelling in the power generation field. It maintains balance among components, subsystems, and the entire system while ensuring mass and energy conservation. In this software, a thermodynamic cycle is constructed from a non-linear system of equations, solved iteratively through a series of linear equations, and variable coefficients are formed using the previous iteration values. The iteration stops when the basic variable no longer changes. Before and after integration, the input of biomass fuel remains constant (considered as 100%), and the losses of biomass boilers remain unchanged. The 8.26 MWh of solar energy is input into the integrated system, and the exhaust steam volume increases with the decrease of heating extraction volume. The thermal losses of steam turbines, condensers, and generators all increase. In addition, due to the heat resource of solar heating system, the heat loss of heating grid system was reduced by 1.77 MW/h, while the heat loss of solar heating system was reduced by 7.35 MW/h. Overall, the power loss of the entire system has increased by 6.49 MWh. Meanwhile, the total output has increased by 1.79 MWh. Although the overall efficiency has decreased by 0.22%, the photoelectric conversion efficiency can reach 21.61%.

## References

- [1] Ono, A., *et al.*, Fundamental Analysis Of Vorticity With Thermodynamic Effect For Early Detection Of Heavy Rainfall Occurrence, *Journal of Japan Society of Civil Engineers, Ser. B1 (Hydraulic Engineering)*, 77 (2021), 2, pp. I\_1129-I\_1134
- [2] Li, D., *et al.*, Investigation of the Explosion Characteristics of Ethylene-Air Premixed Gas in Flameproof Enclosures by Using Numerical Simulations, *Thermal Science*, 27 (2023), 2B, pp. 1573-1586
- [3] Ghodbane, M., *et al.*, Performance Analysis of a Solar-Driven Ejector Air Conditioning System under El-Oued Climatic Conditions, Algeria, *Journal of Thermal Engineering*, 7 (2021), 1, pp. 172-189
- [4] Hao, Z., *et al.*, Performance Optimization of High-Temperature Heat Pump System for Staged Heating under Large Temperature Span, *IOP Conference Series: Earth and Environmental Science*, 766 (2021), 1, 012010
- [5] Yang, J., *et al.*, Thermodynamic Modelling and Real-Time Control Strategies of Solar Micro Gas Turbine System with Thermochemical Energy Storage, *Journal of Cleaner Production*, 304 (2021), 1, 127010
- [6] Kayumova, D. B., *et al.*, Thermodynamic Characteristics of Lithium Pivalate According to High-Temperature Mass Spectrometry Data, *Russian Journal of Inorganic Chemistry*, 66 (2021), June, pp. 868-873
- [7] Salina, V. A., *et al.*, Thermodynamic Simulation of the Carbothermic Reduction of Chromium from the  $\text{Cr}_2\text{O}_3\text{-FeO-CaO-SiO}_2\text{-MgO-Al}_2\text{O}_3$  Oxide System, *Russian Metallurgy (Metally)*, 2021 (2021), 2, pp. 229-233
- [8] Al-Rubaye, L. A. H., *et al.*, Characteristics Study of Gas Turbine Performance with Using Surface Geothermal Energy: Case Study of Iraq, *IOP Conference Series: Materials Science and Engineering*, 1076 (2021), 1, 012069
- [9] Liu, J., *et al.*, Combined with the Residual and Multi-Scale Method for Chinese Thermal Power System Record Text Recognition, *Thermal Science*, 23 (2019), 5A, pp. 2361-2640
- [10] Zhao, B., Analysis of Propagation Characteristics of Hydrogen flame in Shock Tube in Integrated Energy System, *Thermal Science*, 27 (2023), 2A, pp. 1059-1066